A Passivity-based inner-loop Torque Control of Physically Damped Series Elastic Actuators with outer-loop PD Control

Min Jun Kim, Alexander Werner, Florian Loeffl and Christian Ott

***Abstract*— To realize compliant behavior of link-side dynamics of elastic actuators, inner-loop torque control has to generate and deliver PD action to the link-side inertia. However, under this cascade configuration, stability of the overall system is questionable. To solve this problem, this paper presents a guideline for gain selection that ensures stability of the overall cascaded system by passivity. Moreover, passivity has another advantage that it allows us to include the passive environmental interaction into the formulation. The importance of the passivity-based design is addressed by motivating example, and the viability of the proposed approach is verified through the experiments.**

I. Introduction

Soft robotics is one of the major trends in robotics. While some soft behavior can be realized through torque sensing and control, intrinsic compliance enables even more robust behavior. Series-elastic actuators (SEAs) are becoming more and more popular in many robotic applications because they combine torque sensing and mechanical robustness [1]–[5]. Joint torque control of SEA is one of the important research areas as it allows to generate arbitrary link-side behavior (Fig. 1). Common applications like PD control can be implemented in a cascade with a torque control loop, shaping the intrinsic behavior, if necessary [6], [7].

A number of approaches to implement SEA torque control were previously presented [8]–[12]. In all applications, the generation of link-side damping requires acceleration feedback which has a significant impact on stability. In practical applications this limitation may be huge especially when the system is exposed to collisions with the environment, e.g. in bipedal walking [13]. Our previous work [14] shows that this limitation can be overcome by adding physical damping in parallel to the elastic element. Conceptually speaking, this new intrinsic viscous damping lowers the relative degree of the joint torque to the system input to one, and therefore a simple PI control is acceptable for physically damped SEA (pdSEA) systems. As this does not any more require acceleration feedback, the controlled system is robust against impacts on the link side.

Additional advantages of adding physical damping has been studied in [15] (see also [16]–[20]). For example,

All authors are with the Institute for Robotics and Mechatronics, German Aerospace Center (DLR). E-mail address <firstname>.<lastname>@dlr.de.

This work was supported by the Helmholtz Association (VH-NG-808).

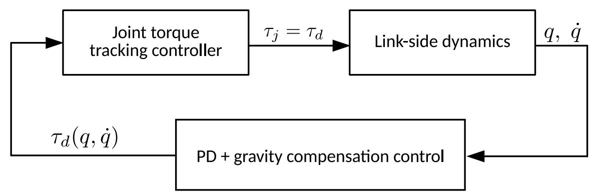

Fig. 1. Overview of the control scheme. Inner-loop joint tracking torque control is cascaded by the outer-loop PD controller.

physical damping may improve the energy efficiency, especially at high frequencies, and control bandwidth. To allow intrinsic motions as well as highly damped applications, variable damping designs have been proposed in literature [17], [20], [21]. Development of this concept and the associated hardware are motivated by the perceived imbalance of actuator weight and link-side performance that can be generated on our SEA-based robot C-Runner [13]. As periodic motions are common in locomotion, the use of intrinsic dynamics is desirable. We expect this development to contribute to increasing the maximum capabilities of the robot in terms of locomotions speed as well as control efficiency. To allow intrinsic motions as well as highly damped applications, variable damping designs have been proposed in literature [17], [20], [21]. A SEA augmented by variable physical damping is called variable physical damping actuator (VPDA) [21].

In the control point of view, VPDA and pdSEA (i.e. fixed damping) are the same under the reasonable assumption that the variability of damping can be neglected in the inner-loop controller because the inner-loop controller has smaller time constants than the damping variation which is determined by the application. Namely, the control concept proposed in our previous work [14] can be directly applied. However the stability properties of the cascaded structure of PD control and torque control were not completely addressed in [14].

Therefore, in this paper, we propose a passivity-based joint torque controller for VPDAs with robust stability. Because VPDA can clearly be advantageous for applications in soft robotics, e.g. human-robot interaction, passive behavior is essential to establish the safety of the control concept. This paper provides a sufficient condition for control gains to satisfy passivity. A motivating example underline that VPDA-based systems can have unstable behavior when passivity conditions are not met, whereas the system is stable under the proposed

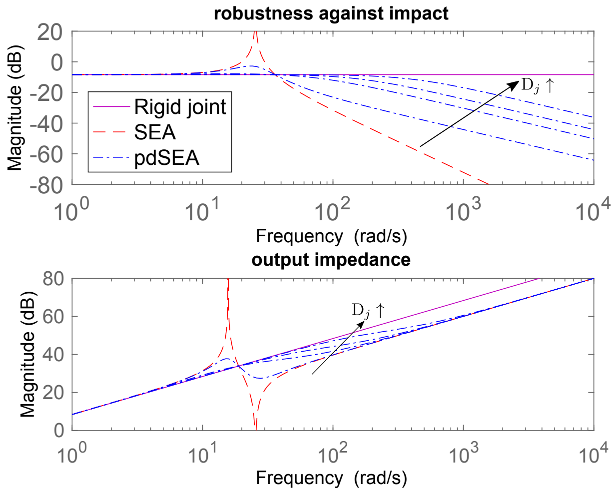

Fig. 2. Top: magnitude bode plot for (1). Bottom: the plot for (2). Physically damped SEA is a combination of SEA and rigid joint robots, but more likely to behave like rigid joint robot, as D_j grows. This is obvious from physical sense because higher damping makes the joint coupling stronger.

control design. Additionally we verify the viability of the approach in the experiment, including environment collision and interaction.

This paper is organized as follows. In Section II, the benefits of physical damping are reviewed, and problem addressed in this paper is described using a motivating example. Section III describes the gain tuning guideline to ensure the passivity. In Section IV, the proposed scheme is verified through experiments. Section V concludes the paper.

II. Motivation

A. Adding joint damping in addition to the elasticity

Although SEA systems have advantages such as robustness against impact and low output impedance, it also has disadvantages especially for the joint torque control capabilities, as pointed out in [14]. Physically speaking, this is because the elastic element decouples motor-side and the link-side inertias. The motor inertia has to be accelerated quickly enough to deliver torque generated by the motor to the link inertia. In contrast, damper strengthens the coupling between motor and link inertia, so it helps delivering the torque generated by the motor to link inertia, similar to rigid joint robot case.

The characteristics of pdSEA lies somewhere in the middle of rigid joint and SEA. This is mathematically clear if we investigate the transfer functions. For example, the open-loop transfer function of external torque to the motor acceleration (which can be interpreted as robustness against impact) is

$$\ddot{\theta}(s) = \frac{D_j s + K_j}{BMs^2 + D_j(M+B)s + K_j(M+B)} \tau_{ext}(s) \quad (1)$$

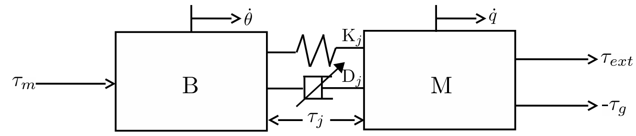

Fig. 3. Schematic diagram of VPDA. M: Link-side inertia, B: Motor-side inertia, τ_m: motor torque, τ_j: joint torque, τ_g: gravity torque, τ_{ext}: external torque acting on the link inertia, K_j: joint stiffness, D_j: joint damping, θ: motor position, and q: link position.

and that of output impedance is

$$\tau_{ext} = \frac{BMs^3 + D_j(M+B)s^2 + K_j(M+B)s}{Bs^2 + D_j s + K_j} \dot{q}(s), \quad (2)$$

where the parameters are introduced in Fig. 3. Note that (1) and (2) become rigid joint as $D_j \to \infty$, and become SEA if $D_j = 0$. Magnitude plots with various parameters are shown in Fig. 2, and it is clear that the pdSEA is somewhere in the middle of rigid joint and SEA depending on D_j. Please refer to [15] for more detailed discussions on the characteristics of pdSEAs.

Note that the implementation of variable damping is relatively easy and weight efficient compared to variable stiffness design. Moreover the damping can be adjusted nearly instantaneously as no energy input is required because it has no (little) dynamics, whereas the online tuning of stiffness is not easy because of the its own dynamics. In other words, it is possible to change the system characteristics from near-SEA to near-rigid joint while the system is running.

B. Joint torque control of variable physically damped SEA

A schematic diagram of VPDA is shown in Fig. 3. The equation of motion is given by

$$M(q)\ddot{q} + C(q,\dot{q})\dot{q} = \tau_j - \tau_g(q) \quad (3)$$

$$B\ddot{\theta} + \tau_j = \tau_m \quad (4)$$

with

$$\tau_j = K_j(\theta - q) + D_j(\dot{\theta} - \dot{q}). \quad (5)$$

By taking a time derivative, we have

$$\dot{\tau}_j = K_j(\dot{\theta} - \dot{q}) + D_j(B^{-1}(\tau_m - \tau_j) - \ddot{q}). \quad (6)$$

Note that, to be precise, $\dot{D}_j$ should be taken into account, but it can be assumed to be zero because the inner loop runs in high frequency (3 kHz in our setup), and D_j varies slowly in view of inner loop controller.[1] Under this assumption, VPDA and pdSEA are the same in the control point of view. For this reason, only VPDA will be considered hereinafter because it includes pdSEA.

Although (6) forms a torque dynamics having input τ_m in the equation, compensation of $K_j(\dot{\theta} - \dot{q})$ is needed if we design a controller using (6). In order to avoid

[1] Or, $\dot{D}_j(\dot{\theta} - \dot{q})$ can be simply eliminated by feedback.

unnecessary feedback cancellations, we take one more derivative:

$$\ddot{\tau}_j = K_j(B^{-1}(\tau_m - \tau_j) - \ddot{q}) + D_j(B^{-1}(\dot{\tau}_m - \dot{\tau}_j) - \dddot{q}). \tag{7}$$

Using

$$\tau_m = Bu + \tau_j + B\ddot{q}, \tag{8}$$

(7) reduces to

$$\ddot{\tau}_j = K_j u + D_j \dot{u}. \tag{9}$$

Here, in terms of stability, D-control is unavoidable for SEA systems, but D-control is not required for VPDA systems because $D_j\dot{u}$ generates D-action from P-control [14].

Now, let us consider a PI joint torque tracking control given by

$$u = L_p e_\tau + L_i \int e_\tau, \tag{10}$$

where $e_\tau = \tau_d - \tau_j$ is the torque error. Substituting this into (9), we obtain

$$\tau_j(s) = \frac{D_j L_p s^2 + (K_j L_p + D_j L_i)s + K_j L_i}{s^3 + D_j L_p s^2 + (K_j L_p + D_j L_i)s + K_j L_i}\tau_d(s) \tag{11}$$

meaning that the resulting τ_j is the low-pass filtered signal of τ_d.

Stability of the overall cascaded system, however, is unclear. To solve stability issues, we propose a passivity-based approach in this paper. In fact, passivity property has great advantage in VPDA applications because it allows us to include passive environmental interaction in the analysis.

Remark 1 (Torque controller in [14]): The proposed controller in [14] was designed using (6), so it had compensation of $K_j(\dot{\theta} - \dot{q})$ in τ_m. Other than this, it had $\dot{\tau}_d$ feed-forward to make the closed-loop torque error dynamics exponentially stable. The stability of overall system could be made on top of exponential tracking of desired torque. However, in practice, if exponential tracking fails (for example, due to the environmental interaction), then the stability becomes questionable. Moreover, $\dot{\tau}_d$ implies acceleration feedback which is amplified by D-control gain of outer-loop controller. To avoid this, this paper does not consider $\dot{\tau}_d$ feed-forward in the control law.

Remark 2 (Feedforward of $B\ddot{q}$): It should be to mentioned that, although $\ddot{q}$ should be calculated numerically, feed-forward term $B\ddot{q}$ in τ_m may not be harmful in practice because it is not amplified by any control gains. An alternative is to use $\ddot{q} = M^{-1}(-C\dot{q} + \tau_j - \tau_g + \tau_{ext})$ from (3). Because τ_{ext} is not known, we can simply treat it as a disturbance. The important remark is that, whatever method we choose, the compensation of $\ddot{q}$ is important to achieve high performance joint torque tracking, because of so-called natural velocity feedback effect [8], [22], [23].

TABLE I
TWO SETS OF GAINS USED IN THE MOTIVATING EXAMPLE

Description	Symbol	Value
Gain Set 1	σ	10
	L_p	$\sigma = 10$
	L_i	$\sigma^2 = 100$
Gain Set 2	σ	$100^{1/3}$
	L_p	$\sigma^2 = 21.5443$
	L_i	$\sigma^3 = 100$

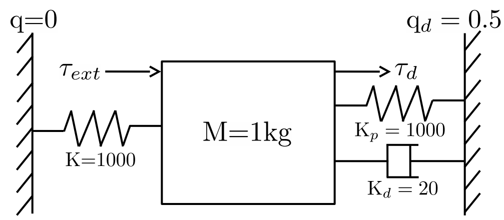

Fig. 4. Motivating example. PD control is applied to the mass m which is connected with the environment by spring.

C. Motivating example

To impact the necessity of passivity-based design, we present a motivating example.

Consider a single degree of freedom case with $M = 1$ kg, $C = 0$, $\tau_g = 0$, $B = 1.62$ kg, $K_j = 400$ N/m, $D_j = 10$ Ns/m in (3)-(5). The following outer-loop PD control is applied to the link side mass.

$$\tau_d = \underbrace{K_p(q_d - q) - K_d\dot{q}}_{=\tau_{pd}} + \underbrace{0}_{=\tau_g}, \tag{12}$$

where the new notation τ_{pd} and τ_g are introduced for consistency with the later part of the paper. The parameters are $K_p = 1000$ N/m, $K_d = 20$ Ns/m, and the desired trajectory is $q_d = 0.5$ m (set-point). In addition, the link-side is coupled with environment by a spring (i.e. passive) of which stiffness is 1000 N/m, as described in Fig. 4. Hence, the mass should converge to $q = 0.25$ m.

To realize this outer-loop control, inner-loop torque control (8) with (10) is applied for two sets of gains listed in Table I. Note that these two gain sets are the same except for the P-gains. Both gains showed similar torque tracking results for a sinusoidal test signal $\tau_d = 10\sin(4\pi t)$. Nevertheless, when the PD control and environmental interaction are taken into account, the resulting behaviors were very different. The controlled system was unstable for the gain set 1 (Fig. 5b), whereas it was stable for the gain set 2 (Fig. 5c).

In conclusion, this motivating example shows that the overall system's stability could be affected by small variation of control gains. In the following section, we propose a gain selection rule to stabilize the controlled system based on the passivity theory.

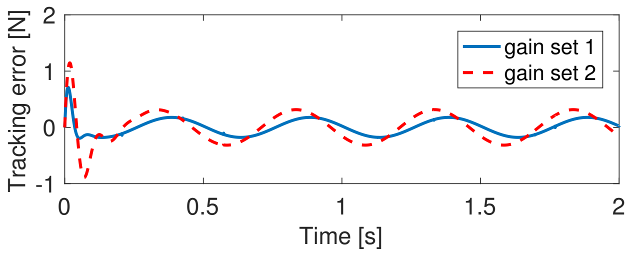

(a) Torque tracking error for sinusoidal desired torque

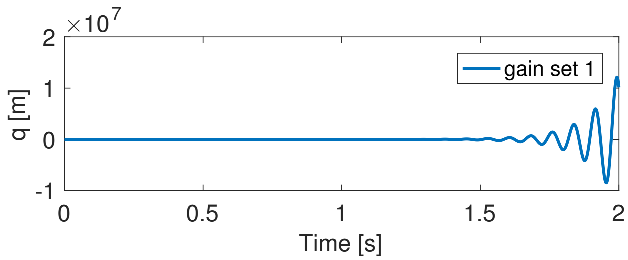

(b) Simulation result using gain set 1

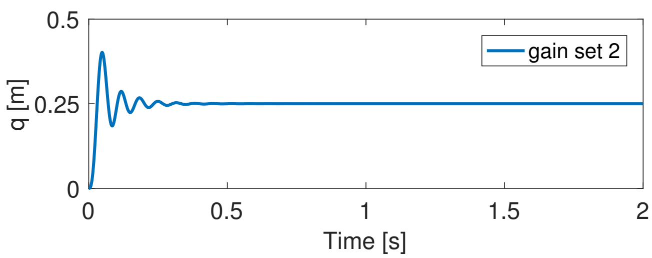

(c) Simulation result using gain set 2

Fig. 5. Simulation result for the motivating example. Both sets of gains tracks sinusoidal test input reasonably. However, when the PD control and environmental interaction is considered as shown in Fig. 4, the gain set 1 did not stabilize the system, whereas the gain set 2 stabilized it.

III. Passivity-Based Control Design

Let us consider a general form of outer-loop PD controller

$$\tau_d = \underbrace{K_p(q_d - q) + K_d(\dot{q}_d - \dot{q})}_{=\tau_{pd}} + \tau_g. \tag{13}$$

To realize this outer-loop controller, define an inner-loop torque tracking control law by

$$\tau_m = Bu + Bu_g + \tau_j + B\ddot{q} \tag{14}$$

with[2]

$$u_g = \frac{s^2}{D_j s + K_j}\tau_g \tag{15}$$

and

$$u = L_p e_\tau + L_i \int e_\tau \tag{16}$$

[2]In practice, u_g usually has small value because it can be rewritten as $\frac{1}{K_j}\left(\frac{K_j/D_j}{s+K_j/D_j}\ddot{\tau}_g\right)$. Namely, $\ddot{g}(q)$ is divided by K_j (which has at least 10^2 order usually) after low-pass filtering.

which is identical to (10), but rewritten for the readers' convinience. Fig. 6 summarizes the overall scheme with

$$C_q(s) = \frac{K_d s + K_p}{s}, \quad C_\tau(s) = \frac{L_p s + L_i}{s}, \quad P_\tau(s) = \frac{D_j s + K_j}{s^2}. \tag{17}$$

The transfer function from $\dot{q}_d - \dot{q}$ to $\tau_j - \tau_g$ is[3]

$$\frac{\tau_j - \tau_g}{\dot{q}_d - \dot{q}} = \frac{(K_d s + K_p)\left(D_j L_p s^2 + (K_j L_p + D_j L_i)s + K_j L_i\right)}{s\left(s^3 + D_j L_p s^2 + (K_j L_p + D_j L_i)s + K_j L_i\right)} \tag{19}$$

For simplicity, define the control gains by $L_p = \sigma^{n_p}$ and $L_i = \sigma^{n_i}$, where σ is a new control gain and $n_p, n_i > 0$ are some constants. The following Theorem tells us about the positive realness of (19).

Theorem 1 (Positive realness of (19)): Assume that the orders of $L_p, L_i > 0$ satisfy

$$2n_p > n_i. \tag{20}$$

Then, (19) is a positive real transfer function for sufficiently large σ.

Proof: To show (19) is positive real, we have to show that (i) (19) is stable, and (ii) the real part of (19) with $s = jw$ is positive for all w.

For (i), stability is trivial from Routh Hurwitz criterion under the constraint (20).

For (ii), the real part can be obtained as

$$\mathbb{R}\left(\frac{\tau_j - \tau_g}{\dot{q}_d - \dot{q}}(jw)\right) = \frac{1}{den}\left(a_6 w^6 + a_4 w^4 + a_2 w^2\right), \tag{21}$$

with

$$a_6 = D_j^2 K_d L_1^2 - (D_j K_p + K_j K_d)L_1 - D_j K_d L_2, \tag{22}$$
$$a_4 = D_j^2 K_d L_2^2 + K_j^2 K_d L_1^2 + K_j K_p L_2, \tag{23}$$
$$a_2 = K_j^2 K_d L_2^2. \tag{24}$$

To a_6 be positive, the highest order should be $2n_p$, and this should be larger than n_p (which is trivial) and n_i. Hence the constraint (20) follows. a_4 and a_2 are always positive. ■

The following Corollaries are consequence of this Theorem.

Corollary 1 (Asymptotic stability): Assume that $\dot{q}_d = 0$ and $\tau_{ext} = 0$. If Theorem 1 holds, then the controlled system is asymptotic stable to $\tau_j = \tau_g(q_d)$ and $q = q_d$.

Proof: To find an equilibrium point, by plugging (14)-(16) into (7), we have

$$\ddot{e}_\tau + D_j L_p \dot{e}_\tau + (K_j L_p + D_j L_i)e_\tau + K_j L_i \int e_\tau = -\ddot{\tau}_{pd}. \tag{25}$$

[3]For readers' information, the closed-loop torque dynamics is

$$\tau_j = \frac{D_j L_p s^2 + (K_j L_p + D_j L_i)s + K_j L_i}{s^3 + D_j L_p s^2 + (K_j L_p + D_j L_i)s + K_j L_i}\tau_{pd} + \tau_g. \tag{18}$$

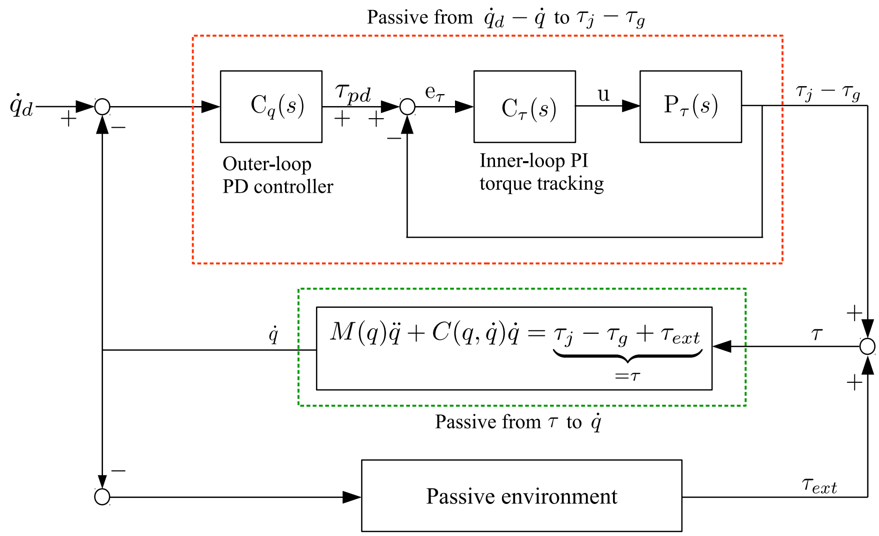

Fig. 6. Overall control structure. If the upper part (red dotted) is passive from $\dot{q}_d - \dot{q}$ to $\tau_j - \tau_g$, then the overall control structure can be constructed by feedback interconnections of passive subsystems. C_q, C_τ, P_τ are defined by (17).

In steady state, $\dot{e}_\tau = 0$, $e_\tau = 0$, $\int e_\tau = 0$ (note that the integration converges to disturbance, if any) with $\tau_d = K_p(q_d - q) + \tau_g(q)$, and $\tau_g(q) = \tau_j$. Combining all these, the unique equilibrium point is $\tau_j \equiv \tau_g(q_d)$, $q \equiv q_d$.

Because the transfer function from $-\dot{q}$ to $\tau_j - \tau_g$ is positive real, positive real lemma [24] says that there exists a positive definite storage function $S(x)$ which satisfies $\dot{S}(x) \leq -\dot{q}^T(\tau_j - \tau_g)$, where x is a state for the transfer function. Define the Lyapunov function by $V(q, \dot{q}, x) = S(x) + \frac{1}{2}\dot{q}^T M(q)\dot{q}$. Because $\dot{V} \leq 0$, the asymptotic stability can be concluded by the invariance principle. ■

Corollary 2 (Passivity): If Theorem 1 holds, then the overall control structure in Fig. 6 can be constructed by feedback interconnections of passive subsystems. Hence, as long as $\dot{q}_d$ is $\mathcal{L}_2$ signal, the controlled system is asymptotically stable.

Proof: Positive real of (19) implies passivity of the input-output pair $(\dot{q}_d - \dot{q}, \tau_j - \tau_g)$. The rest is trivial. ■

Finally, we remark the followings.

Remark 3 (Gain tuning guideline): Theorem 1 provides a guideline for selecting PI gains that, when tuning the PI gains, I gain should not be increased faster than square of P gain. In other words, when the user increases P gain by double, I gain should not increase more than factor 4. In this paper, as an example, we use the following gain tuning rule:

$$L_p = \sigma^2 \text{ and } L_i = \sigma^3. \tag{26}$$

Remark 4 (Practical constraints on K_p, K_d, and D_j): Although Theorem 1 is true for sufficiently large σ, in practice, achievable σ is limited. By plugging (26) into (23), we obtain

$$a_6 = D_j K_d \left(D_j \sigma^2 - \sigma - (\frac{K_p}{K_d} + \frac{K_j}{D_j}) \right) \sigma^2. \tag{27}$$

From this, we have the following observations:

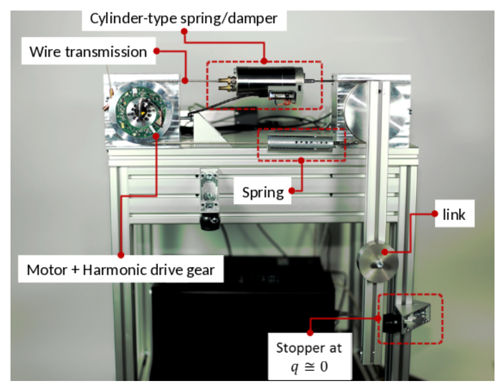

Fig. 7. Experimental setup. The left and right discs (i.e. motor- and link- side inertias, respectively) are connected by a steel cable. A joint module from DLR LWR with 1:100 gear ratio is used. In the transmission, the upper element is explained in Fig. 8, and the lower one is a steel spring. An end-stop is located at $q \simeq 0$.

- Achievable D_j should be lower bounded properly. In our setup, it is lower bounded by 4 $\mathrm{Nm \cdot s/rad}$.
- $\frac{K_p}{K_d}$ should be upper-bounded properly. Namely, too small K_d is not allowed.

Otherwise, too larger σ may be required.

Remark 5 (Revisiting the motivating example): Note that the gain set 1 in Table I does not meet the constraint (20), meaning that the resulting controller may not be passive. Due to the lack of passivity, the controlled system was unstable. On the other hand, the gain set 2 meets the constraint (20), and therefore the controlled system was stable.

IV. Experiments

Fig. 7 shows the experimental setup. Motor-side inertia and link-side inertia are coupled by spring-damper element. To realize variable damping, a pull type spring/damper was designed, of which cross section is

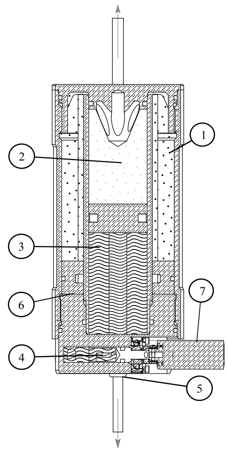

Fig. 8. Cross section of the VPDA with an elastic element formed by the active air chamber (1) and the linearizing air chamber (2), connected by the hydraulic system (3)(6) with the variable throttle valve (4) providing viscoelastic behavior on the piston rod (5) A mini servo (7) sets the damping throttle.

shown in Fig. 8 . Elastic spring behavior is implemented by a two chamber air spring generating almost linear spring characteristics. The damping part is taken over by a hydraulic piston-throttle combination, regulating the oil flow between the two oil chambers. With this design the damping can be adjusted fast and with low forces. A tiny servo drive works fine in this system, tuning the damping from fully closed to fully open takes less than 0.05 s.

In the experiments, The PD control is applied with $K_p = 100$ Nm/rad and $K_d = 20$ Nm $\cdot$ s/rad with $q_d = -0.075 \sin(2\pi t)$ rad. The amplitude 0.075 was selected to avoid motor saturation. During the motion, the damping value is changes by $D_j = 30 + 25 \sin(\pi t)$ Nm $\cdot$ s/rad as shown in Fig. 9a.

In the first experiments (Fig. 9b), similar to the motivating example, the link was clamped at $q \simeq 0$ (note that clamping can be considered as a spring connection to $q \simeq 0$ which has very high stiffness). Although q could not move because of the clamping, the controlled system was stable.

In the second experiment (Fig. 9c), to make the system more dynamic, link clamping was eliminated. However, there was still an environmental interaction (collision) at the end-stop (namely, q cannot move further than $q \simeq 0$). It is interesting to observe that, the exact torque tracking could not be obtained mainly due to the environmental collision. As a consequence of imprecise torque tracking, the correct amount of torque (defined by outer-loop pd plus gravity compensation) could not be delivered to the link-side inertia. Despite this error propagation, the overall system remained stable because the gains were tuned to satisfy passivity.

In the third experiment (Fig. 10), strong impact at the end-stop was intentionally made to see the effectiveness of VPDA. To make periodic impacts using the PD

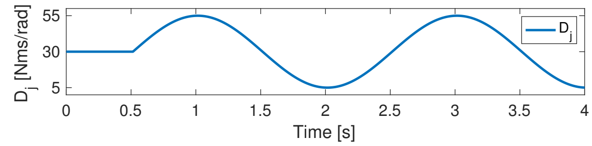

(a) Damping variation during the experiment

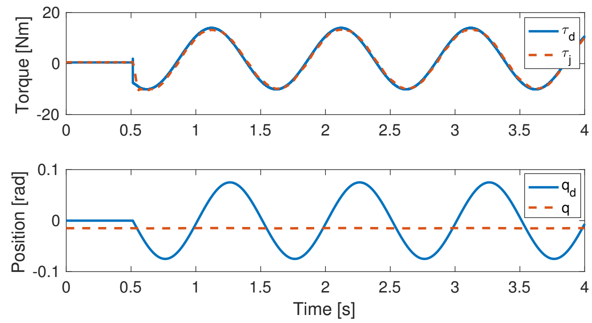

(b) The link was clamped $q \simeq 0$

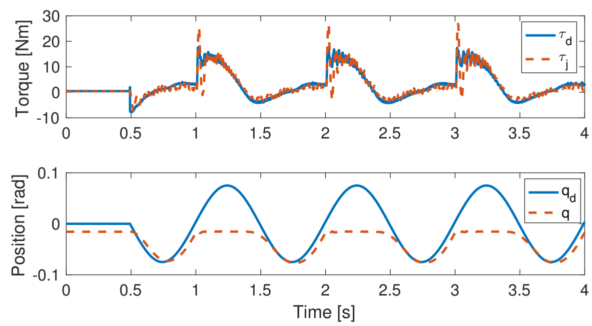

(c) The link was not clamped

Fig. 9. Experimental results with outer-loop PD control. (a) During the experiment, D_j was changed by $D_j = 30 + 25 \sin(\pi t)$. (b) The link-side was clamped at $q \simeq 0$. Note that the clamping can be though of as an environmental interaction. (c) The link was not clamped, but still could not move further than $q \simeq 0$ because of the end-stop (Fig. 7). The link inertia collided at the end-stop.

control, q_d was set as a pulse signal with peak values of -0.3 rad and 0.3 rad. Please note that q did not track q_d because the motor hits saturation, and the purposed of this experiment was not to track q_d, but to make an periodic impact at the end-stop. Initially, D_j was 50 Nm $\cdot$ s/rad, and it was changed to 5 Nm $\cdot$ s/rad at $t = 4$s. When the D_j was set 50, the measured impact torque was 65.23 Nm, and it was reduced to 45.2 Nm when $D_j = 5$ Nm $\cdot$ s/rad. This is physically clear that higher D_j makes the system behave more like a rigid joint, and lower D_j makes the system behave more like a SEA. From this experiment, we confirmed that the VPDA can change system characteristics by utilizing variable damping.

V. Conclusion and Future Works

To apply PD control to the link-side of physically damped series elastic actuators (pdSEAs) or variable physical damping actuators (VPDAs), cascading of inner-loop PI torque tracking control (followed by feed-forward input) is a straightforward solution. However,

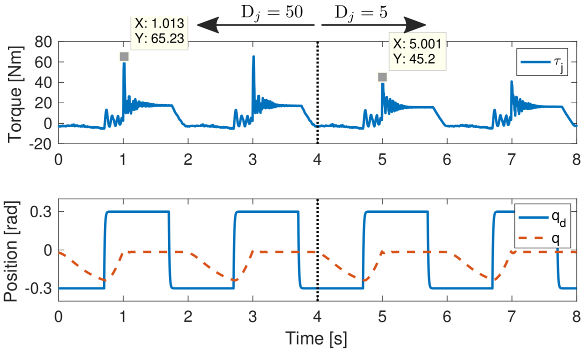

Fig. 10. Experimental result for impact test. To make periodic impact, q_d was defined as a periodic pulse signal. D_j was 50, and was changed to 5 at $t = 4$s. The measured impact torque was reduced when D_j was lowered because it weakens the coupling. Namely, the system behaved more like a SEA system.

under this cascade configuration, stability of the overall system is questionable. Furthermore, stability analysis becomes more difficult when the environmental interaction, which is motivation for pdSEA- and VPDA- based systems, is taken into account.

Passivity can be a key ingredient for stability of the overall system, because it allows us to include passive environmental interaction in the analysis by little extension. This paper claims that, when tuning the inner-loop PI controller, the I gain should not increase faster than the square of P gain to ensure the passivity. The motivating example shows that the controlled system may not be stabilized when this condition is not met, whereas the controlled system is stable under the sufficient condition. Experiment shows the viability of the proposed approach on real hardware.

We plan to apply this concept to our SEA robot C-Runner [13]. As stated earlier, we expect an increase of the capabilities in terms of locomotion speed and control efficiency.

References

[1] M. Zinn, O. Khatib, B. Roth, and J. K. Salisbury, "Playing it safe [human-friendly robots]," *Robotics & Automation Magazine, IEEE*, vol. 11, no. 2, pp. 12–21, 2004.

[2] S. Haddadin, F. Huber, and A. Albu-Schäffer, "Optimal control for exploiting the natural dynamics of variable stiffness robots," in *Robotics and Automation (ICRA), 2012 IEEE International Conference on*. IEEE, 2012, pp. 3347–3354.

[3] K. Kong, J. Bae, and M. Tomizuka, "A compact rotary series elastic actuator for human assistive systems," *Mechatronics, IEEE/ASME Transactions on*, vol. 17, no. 2, pp. 288–297, 2012.

[4] J. Arata, K. Ohmoto, R. Gassert, O. Lambercy, H. Fujimoto, and I. Wada, "A new hand exoskeleton device for rehabilitation using a three-layered sliding spring mechanism," in *IEEE International Conference on Robotics and Automation (ICRA)*, 2013, pp. 3902–3907.

[5] M. J. Kim and W. K. Chung, "Disturbance-observer-based pd control of flexible joint robots for asymptotic convergence," *Robotics, IEEE Transactions on*, vol. 31, no. 6, pp. 1508–1516, 2015.

[6] C. Ott, A. Dietrich, and A. Albu-Schäffer, "Prioritized multi-task compliance control of redundant manipulators," *Automatica*, vol. 53, pp. 416–423, 2015.

[7] J. H. Kim, S.-m. Hur, and Y. Oh, "Maximum tracking errors in pd-controlled robotic manipulators," in *System Integration (SII), 2016 IEEE/SICE International Symposium on*. IEEE, 2016, pp. 676–681.

[8] T. Boaventura, M. Focchi, M. Frigerio, J. Buchli, C. Semini, G. A. Medrano-Cerda, and D. G. Caldwell, "On the role of load motion compensation in high-performance force control," in *IEEE/RSJ International Conference on Intelligent Robots and Systems (IROS)*, 2012, pp. 4066–4071.

[9] S.-m. Hur, S.-R. Oh, and Y. Oh, "Joint space torque controller based on time-delay control with collision detection," in *IEEE/RSJ International Conference on Intelligent Robots and Systems (IROS)*, 2014, pp. 4710–4715.

[10] S. Yoo and W. K. Chung, "Sea force/torque servo control with model-based robust motion control and link-side motion feedback," in *IEEE International Conference on Robotics and Automation (ICRA)*, 2015, pp. 1042–1048.

[11] N. Paine, J. S. Mehling, J. Holley, N. A. Radford, G. Johnson, C.-L. Fok, and L. Sentis, "Actuator control for the nasa-jsc valkyrie humanoid robot: A decoupled dynamics approach for torque control of series elastic robots," *Journal of Field Robotics*, vol. 32, no. 3, pp. 378–396, 2015.

[12] W. Lee, M. J. Kim, and W. K. Chung, "Model-free joint torque control strategy for hydraulic robots," in *IEEE International Conference on Robotics and Automation (ICRA)*, 2016, pp. 2408–2415.

[13] F. Loeffl, A. Werner, D. Lakatos, J. Reinecke, S. Wolf, R. Burger, T. Gumpert, F. Schmidt, C. Ott, M. Grebenstein, *et al.*, "The dlr c-runner: Concept, design and experiments," in *Humanoid Robots (Humanoids), 2016 IEEE-RAS 16th International Conference on*. IEEE, 2016, pp. 758–765.

[14] M. J. Kim, A. Werner, F. Loeffl, and C. Ott, "Enhancing joint torque control capability of series elastic actuators with physical damping (accepted)," in *IEEE International Conference on Robotics and Automation (ICRA)*, 2017.

[15] M. Laffranchi, L. Chen, N. G. Tsagarakis, and D. G. Caldwell, "The role of physical damping in compliant actuation systems," in *Intelligent Robots and Systems (IROS), 2012 IEEE/RSJ International Conference on*. IEEE, 2012, pp. 3079–3085.

[16] C.-M. Chew, G.-S. Hong, and W. Zhou, "Series damper actuator: a novel force/torque control actuator," in *4th IEEE/RAS International Conference on Humanoid Robots*, vol. 2, 2004, pp. 533–546.

[17] M. Laffranchi, N. Tsagarakis, and D. G. Caldwell, "A compact compliant actuator (compact$^{\text{TM}}$) with variable physical damping," in *IEEE International Conference on Robotics and Automation (ICRA)*, 2011, pp. 4644–4650.

[18] A. Radulescu, M. Howard, D. J. Braun, and S. Vijayakumar, "Exploiting variable physical damping in rapid movement tasks," in *Advanced Intelligent Mechatronics (AIM), 2012 IEEE/ASME International Conference on*. IEEE, 2012, pp. 141–148.

[19] M. Laffranchi, N. G. Tsagarakis, and D. G. Caldwell, "Analysis and development of a semiactive damper for compliant actuation systems," *IEEE/ASME Transactions on Mechatronics*, vol. 18, no. 2, pp. 744–753, 2013.

[20] B. Vanderborght, A. Albu-Schäffer, A. Bicchi, E. Burdet, D. G. Caldwell, R. Carloni, M. Catalano, O. Eiberger, W. Friedl, G. Ganesh, *et al.*, "Variable impedance actuators: A review," *Robotics and autonomous systems*, vol. 61, no. 12, pp. 1601–1614, 2013.

[21] M. Laffranchi, N. G. Tsagarakis, and D. G. Caldwell, "A variable physical damping actuator (vpda) for compliant robotic joints," in *Robotics and Automation (ICRA), 2010 IEEE International Conference on*. IEEE, 2010, pp. 1668–1674.

[22] S. Dyke, B. Spencer Jr, P. Quast, and M. Sain, "Role of control-structure interaction in protective system design," *Journal of Engineering Mechanics*, vol. 121, no. 2, pp. 322–338, 1995.

[23] A. Alleyne and R. Liu, "On the limitations of force tracking control for hydraulic servosystems," *Journal of dynamic systems, measurement, and control*, vol. 121, no. 2, pp. 184–190, 1999.

[24] H. K. Khalil and J. Grizzle, *Nonlinear systems*. Prentice hall Upper Saddle River, 2002, vol. 3.